Cellular Physiology and Biochemistry

Cell Physiol Biochem 2018;46:1159-1174
DOI: 10.1159/000489058
Published online: April 19, 2018
Accepted: March 05, 2018

Original Paper

Metabolic Plasticity Enables Circadian Adaptation to Acute Hypoxia in Zebrafish Cells

Adolf M. Sandbichler[a] Bianca Jansen[a] Bettina A. Peer[a] Monika Paulitsch[a] Bernd Pelster[a] Margit Egg[a]

[a]Institute of Zoology, University Innsbruck, Austria

Key Words
Hypoxia • Circadian clock • Glycolysis • ADP/ATP ratio • Metabolic oscillations • Peroxiredoxin • Cytosolic H_2O_2 oscillation • Redox system • Realignment

Abstract
Background/Aims: Reduced oxygen availability, hypoxia, is frequently encountered by organisms, tissues and cells, in aquatic environments as well as in high altitude or under pathological conditions such as infarct, stroke or cancer. The hypoxic signaling pathway was found to be mutually intertwined with circadian timekeeping in vertebrates and, as reported recently, also in mammals. However, the impact of hypoxia on intracellular metabolic oscillations is still unknown. ***Methods:*** For determination of metabolites we used Multilabel Reader based fluorescence and luminescence assays, circadian levels of Hypoxia Inducible Factor 1 alpha and oxidized peroxiredoxins were semi quantified by Western blotting and ratiometric quantification of cytosolic and mitochondrial H_2O_2 was achieved with stable transfections of a redox sensitive green fluorescent protein sensor into zebrafish fibroblasts. Circadian oscillations of core clock gene mRNA´s were assessed using realtime qPCR with subsequent cosine wave fit analysis. ***Results:*** Here we show that under normoxia primary metabolic activity of cells predominately occurs during day time and that after acute hypoxia of two hours, administrated immediately before each sampling point, steady state concentrations of glycolytic key metabolites such as glucose and lactate reveal to be highly rhythmic, following a circadian pattern with highest levels during the night periods and reflecting the circadian variation of the cellular response to hypoxia. Remarkably, rhythms in glycolysis are transferred to cellular energy states under normoxic conditions, so that ADP/ATP ratios oscillate as well, which is the first evidence for cycling ADP/ATP pools in a metazoan cell line to our knowledge. Furthermore, the hypoxia induced alterations in rhythms of glycolysis lead to the alignment of three major cellular redox systems, namely the circadian oscillations of NAD^+/NADH and $NADP^+$/NADPH ratios and of increased nocturnal levels of oxidized peroxiredoxins, resulting in a highly oxidized nocturnal cellular environment. Of note, circadian rhythms of cytosolic H_2O_2 remain unaltered, while the transcriptional clock is already attenuated, as it is known to occur also under chronic hypoxia. ***Conclusion:*** We therefor propose that the realignment of metabolic redox oscillations might initiate the observed hypoxia induced attenuation of the transcriptional clock, based on the reduced binding affinity of the CLOCK/BMAL complex to the DNA in an oxidized environment.

Margit Egg

Institute of Zoology University Innsbruck
Technikerstr. 25, Innsbruck (Austria)
E-Mail margit.egg@uibk.ac.at

Introduction

Reduced oxygen availability, hypoxia, is frequently encountered by organisms, tissues and cells for various periods of time, in aquatic environments as well as in high altitude mountain areas, under strong physical exercise or in pathological conditions such as infarct, stroke or cancer. The cellular system to cope with reduced oxygen levels, the hypoxic signaling pathway with its major transcription factor Hypoxia Inducible Factor-1 α (HIF-1α) and its isoforms has thus been extensively studied from invertebrates to humans [1-4]. Besides, oxygen deficiency has also been shown to affect another essential pathway, the circadian clock, an interplay which meanwhile has been explored in a couple of physiological and molecular studies [5-15].

The cell intrinsic circadian clock comprises several interconnected transcriptional translational feedback loops (TTFL`s), generated by an array of clock genes and their protein products which lead to endogenous oscillations of approximately 24 hours duration through anti-phasic expression cycles. The core loop of the TTFL is basically formed by the CLOCK/BMAL1 protein heterodimer which occupies DNA binding sites called E-boxes of their counter-players, the period and cryptochrome genes. Increasing their transcription, the gene products of both, the PERIOD and CRYPTOCHROME proteins, heterodimerize in the cytosol of cells and block the activity of the CLOCK /BMAL1 complex upon reentry to the nucleus. With the detection of peroxiredoxin (Prx) oxidation cycles, which cover all features of a cell autonomous time keeper such as regular circadian patterns under constant darkness, entrainability to external cues, temperature compensation and independency from nuclear transcription [16-18], the singularity of the TTFL had to be reconsidered. Prxs are small conserved anti-oxidant enzymes which are able to scavenge reactive oxygen species (ROS) by catalyzing the oxidation of their own conserved cysteine residue with subsequent hyperoxidation to sulphonic acid. However, recent findings suggest that Prx oxidation cycles rather form a clock output based on the circadian rhythms of oxidative metabolism than being themselves a further cell autonomous time keeper [19, 20], and also the relationship between Prx cycles and the TTFL is still unknown. Several other metabolites oscillate with a circadian rhythm as well, are controlled by the TTFL and feed back into the system, such as the cyclic biosynthesis of NAD^+, which is mediated by the rate limiting and clock-controlled enzyme nicotinamide phosphoribosyl transferase (NAMPT) [21, 22], or the oscillating NAD^+/NADH and $NADP^+$/NADPH ratios, which enhance the binding of the CLOCK /BMAL1 complex to the DNA through higher levels of their reduced forms [23]. Models for the obvious crosstalk between metabolic oscillations and the TTFL were proposed by several authors [24-26] and only recently the pentose phosphate pathway (PPP), the main source of NADPH production as reducing equivalent was identified as a major regulator of the TTFL [27]. The influence of hypoxia on the TTFL has been investigated in several vertebrate studies [5, 7, 10, 14, 15] and the HIF-1α mediated dampening of specific core clock gene oscillation amplitudes, first described in zebrafish [10, 28] was specified recently also in mice [14, 15]. Similarly, consequences of the reported link between both pathways for organismic physiology were illustrated in both models, in zebrafish [28] and in mice [5, 15], which stresses the translational impact of the findings and the essential nature of the mutual interaction between the circadian clock and oxygen metabolism.

Due to the enlarged concept of cell intrinsic timekeeping described above we set out to explore the effects of acute hypoxia of two hours, applied immediately before each sampling time point covering a full circadian cycle, on selected metabolic rhythms, focusing on key metabolites of glycolysis and effectors and markers of the cellular redox environment. Using the non-transformed vertebrate zebrafish fibroblast cell line Z3 which is directly light-responsive [29] and a descendant of a day active vertebrate we were able to show that highest glycolytic activity of cells following acute hypoxia exposure for two hours occurs during night times, as opposed to cells under normoxia. As a consequence, the NAD^+/NADH ratio oscillation aligns with the hypoxia induced high amplitude rhythm of the $NADP^+$/NADPH ratio and nocturnal Prx_{ox}, leading to highly oxidized states of the cells during the

night periods. While oscillations of canonical clock genes are already dampened after short time hypoxic incubation as it is also known from experiments with chronic hypoxia [10, 14, 15, 28, 30], circadian rhythms of cytosolic H_2O_2 remain absolutely unaffected by the hypoxia induced metabolic and transcriptional changes, implicating that a cellular timekeeping mechanism apart from the transcriptional clock is quite robust against the stress of reduced oxygen tensions. The hypoxia-induced and mostly Hif-1α driven response observed in cellular metabolic rhythms might thus form the basis for the observed hypoxia induced attenuation of the TTFL, against the background of the reduced binding affinity of the CLOCK /BMAL1 complex to DNA in a highly oxidized cellular environment.

Materials and Methods

Cell culture conditions, experimental setup and sampling

All experiments and samplings were performed under normoxia and after two hours of hypoxia (1% O_2 and 99% N_2) administrated immediately before each sampling time point (Fig. 1, A). Hypoxia has an accumulating effect on the Hif-signaling pathway during the first few hours, which can be derived from the increasing levels of Hif-1α protein with increased duration of the hypoxic treatment. Longer hypoxic incubation times in the range of several days, in turn, lead to reduction of Hif-1α protein levels [30]. In addition, it is established that the transcription factor Hif-1α regulates the TTFL by binding directly to the *period1* and *period2* genes [10, 30], so that accumulating or varying amounts of the hypoxic transcription factor might have time variant effects on the tested circadian systems. Due to this knowledge we decided to select two hours of hypoxic incubation time. For this time span the day time dependent amounts of accumulated Hif-1α protein levels in zebrafish cells are known [10, 28], which also means that hypoxic signaling is definitely switched on, but without leading to a highly and therefore potentially harmful hypoxic metabolism, characterized for example through high levels of produced lactate. Zebrafish Z3 cells were cultured at 25°C in Leibovitz 15 (L-15, Thermo Fisher Scientific, Germany) medium supplemented with 15% fetal calf serum in an atmospheric CO_2 non-humidified cell culture incubator as described previously [10]. Cells were entrained to one additional light/dark cycle of 14/10 prior to the first L/D cycle (14/10) of sampling. Entrainment was accomplished using a light incubator (ICP 500, 5 fluorescent tubes at 15W, 1000 lux; Memmert, Germany). Sampling was performed over three circadian cycles, one L/D cycle of 14/10, followed by two cycles under constant darkness.

Sampling for the determination of metabolites was done in parallel to the sampling of total protein for the Western blots, the latter of which is described in detail in [10] using Z3 cells grown in 100 mm culture dishes (Sarstedt,

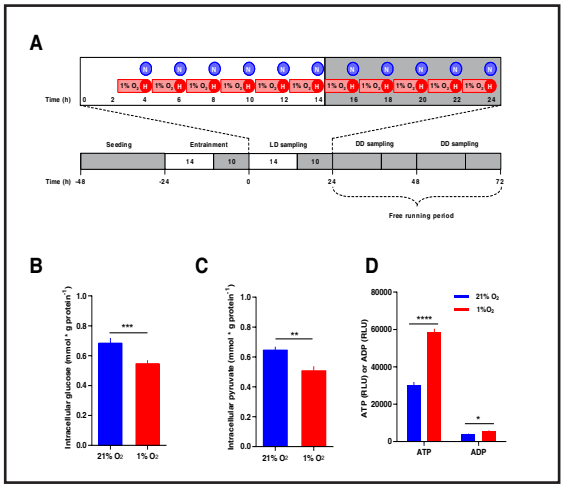

Fig. 1. A: Overview of the light entrainment and sampling schedule. For each sampling time point normoxic (N) and two-hour hypoxia exposed (H) replicates were prepared. The detailed view shows the samplings for one light/dark (LD) sampling day. Two additional sampling days where light-entrained cells were kept under constant darkness were performed to investigate the "free-running period". B and C: intracellular steady state concentrations of glucose and pyruvate, summed up over the two days of constant darkness: hypoxia treated cells have significantly lower amounts of both substrates; D: relative quantities of ATP and ADP, summed up over the two days of constant darkness: hypoxia treated cells have significantly higher ATP and ADP stores compared to normoxic cells; asterisks mark significant differences between the groups; B to G: mean ± SEM; n= 72-132; Two-way ANOVA, Graph Pad Prism 6.

Austria). After decantation of the supernatant/medium, cells were washed with 1x PBS and scraped off in 850µl Tris/EDTA buffer and directly transferred to reaction tubes to get shock frozen in liquid nitrogen. After a centrifugation step at 1000rcf for one minute at 4°C to pellet the cell debris, 10µl aliquots of each sample were set apart for quantification of total protein content using the Nanodrop 2000c Spectrophotometer (Thermo Scientific,Germany). Residual sample volumes were de-proteinated using 10kD molecular weight cut-off Amicon Ultra 0.5 mL centrifugal filters (Merck, Germany) and stored at -80°C until determination of metabolites.

Sampling for cytosolic H_2O_2 measurements was done with identical incubation and sampling timetable but using Z3 cells stably transfected with the cytosolic fluorescent H_2O_2 sensor protein roGFP2-ORP1 and seeded in quadruplicates at a density of 7000 cells per well into individual black 96-well plates (PerkinElmer, Germany). For mitochondrial H_2O_2 measurement Z3 cells stably transfected with a mitochondrial roGFP2-ORP1 sensor protein were seeded on glass coverslips at a density of 50.000 cells per cm^2 and subjected to the same light/dark schedule as all the other samples. One hour before each two-hour normoxic/hypoxic incubation growth media in the wells or in the glass coverslips was exchanged for imaging buffer to reduce autofluorescence. The imaging buffer was a Hank's buffered salt solution containing 5 mM galactose and 5 mM pyruvate and was prepared without glucose to best match the nutrient composition of the growth media L-15.

Western Blots

Isolation and quantification of total cellular protein as well as Hif-1α western blots were performed according to standard procedures described previously [10]. For quantification of peroxiredoxins, membranes were incubated with Prx-$SO_{2/3}$ antibody (ab16830, Abcam, UK) 1:10, 000 in 5% [w/v] bovine serum albumin (BSA) overnight at 4°C, after blocking with 5% [w/v] milk. Binding of the primary antibody was detected with a secondary antibody conjugated to horseradish peroxidase (HRP; Sigma-Aldrich, Germany; diluted 1:1000 in blocking buffer, incubated for 1h at room temperature) using the Amersham™ ECL Prime Western Blotting Detection Reagent (GE Healthcare, UK). Semiquantification of oxidized peroxiredoxins was accomplished by using the Image Lab™ software (Bio-Rad, Germany). The responsiveness of Zebrafish Prx_{ox} protein levels to increasing concentrations of H_2O_2 in the medium is shown in (Fig. 10, C).

Measurement of metabolites

Glucose was measured using the Glucose HK Assay Reagent (Sigma-Aldrich, Germany) and D(+)-Glucose anhydrous (Roth, Germany) for the calibration curves and as standards of known concentrations to carry along with the samples. Measurements were carried out in transparent tissue culture 96 well suspension plates (Sarstedt, Austria) in a Victor X4 2030 Multilabel Reader (PerkinElmer, Germany), according to the manufacturer`s protocol. Lactate and pyruvate concentrations of cells were measured after [31] using the innate fluorescence of NADH versus NAD^+ at an excitation wavelength of 340 nm and an emission wave length of 445 nm [32]. For this purpose calibration curves were generated with the respective salts of known concentrations, sodium L-lactate and sodium pyruvate (Sigma-Aldrich, Germany) between 0 and 1 mM. Measurements were performed in a Victor X4 2030 Multilabel Reader (PerkinElmer, Germany) in 96-well format white culture plates (PerkinElmer, Germany), calibration curves and standards of known concentrations, as well as blanks were carried along with each measurement. Estimations of free cytosolic NAD^+/NADH ratios were calculated according to [33] after determining the equilibrium state of Z3 cells after two hours of hypoxia (Fig. 10, D). For this purpose we transiently transfected Z3 cells seeded into CellASIC Onix M04S live cell imaging plates (Merck Millipore, Germany) with Peredox-mCherry plasmid (#32380, Addgene, USA), a genetically encoded fluorescent NADH-NAD^+ redox sensor [34], using Peqfect DNA transfection reagent (Peqlab VWR, Germany) according to the manufacturer's instructions and previous transfection optimization for zebrafish cells [35]. Several cells in the live cell imaging setup (CellASIC Onix microfluidic perfusion system, Merck Millipore, Germany) were imaged every 2 minutes with a Leica SP5-II laser scanning microscope (Leica Microsystems, Germany) equipped with an automated stage using a 63x objective lens and two excitation wavelengths sequentially detected on a hybrid detector (Ex1 405 nm, Em1 500-550 nm, Ex2 561 nm, Em2 600 – 650 nm). After 20 min of normal air supply the imaging chamber was switched to N_2 for the rest of the experiment. After 140 min the imaging buffer containing 5 mM galactose and 5 mM pyruvate was transiently exchanged for buffer containing 5 mM galactose and 5 mM lactate for another 20 minutes before switching back to the pyruvate containing medium. Ratiometric images were

generated with LAS AF software (version 2.7, Leica Microsystems, Germany). Since no difference in the amount of NADH was detectable in hypoxic cells at 5 mM pyruvate, the formula pyruvate/lactate*9000 ([NAD^+)/[NADH]=[pyr]/[lac]*10^-pH/K_{equ}; K_{equ} of LDH = $1.11*10^{-11}$; pH7) was used for the calculation of NAD^+/NADH ratios. $NADP^+$/NADPH ratios were determined using the $NADP^+$/NADPH-Glo™Assay kit (Promega, Germany). ADP/ATP ratios were determined using the ADP/ATP ratio Assay Kit (Sigma-Aldrich, Germany) according to the protocol provided. For all bioluminescence measurements white 96-well culture plates (Perkin Elmer, Germany) were used in a Victor X4 2030 Multilabel Reader (PerkinElmer, Germany). Measurements of enzyme activities were performed using the Phosphofructokinase (PFK) Activity Colorimetric Assay Kit and the Glucose-6-Phosphate Dehydrogenase Assay Kit (Merck, Germany) according to the protocols provided by the manufacturers.

Realtime qPCR

Realtime qPCR was performed as already published [10, 28].

Ratiometric measurement of H_2O_2 concentrations

Long-term, non-invasive H_2O_2 fluctuations in living cells can be measured with a pH-insensitive H_2O_2 sensor based on a green-fluorescent protein covalently attached to a redox enzyme (Orp1) from *Saccharomyces cerevisiae* [36]. This so-called redox relay with Orp1 effectively converts physiological H_2O_2 signals into measurable fluorescence signals– with higher specificity and kinetics than roGFP2 alone. For cytosolic H_2O_2 measurement a non-targeted version (Fig. 10, A) and for mitochondrial H_2O_2 production a cytochrome oxidase subunit 8 (COX8) targeted version (Fig. 10, B) of roGFP2-Orp1 were successfully introduced into Z3 cells using a retroviral transfection approach. RoGFP2-Orp1 excitation at 405 nm is relatively insensitive to H_2O_2 whereas excitability at 490 nm is H_2O_2-sensitive and results in a strongly reduced emission at 530 nm when the protein is oxidized by H_2O_2. The circadian fluctuation of cytosolic H_2O_2 was assayed with ratiometric roGFP2 fluorescence measurements (Ex1 405 nm, Ex2 488 nm, Em 500 - 550 nm) in a fluorescence plate reader equipped with a monochromator light source (Enspire, Perkin Elmer, Germany). The mitochondrial H_2O_2 in individual Z3 cells was calculated from roGFP2 fluorescence images using a Leica SP5-II laser scanning microscope equipped with hybrid detector and a 63x objective lens. A large 6x5 tile scan at subcellular resolution was recorded with sequential 405 nm or 488 nm excitation and a 500 nm to 550 nm emission band for both excitations. The ratiometric image analysis routine was performed using LAS AF software (version 2.7, Leica Microsystems, Germany). In both setups hypoxia-exposed samples were immediately measured after removal from the hypoxia chamber. Responsiveness of the roGFP2-ORP1 fluorescent protein sensor in the cytosolic or mitochondrial measurement setup was confirmed by applying either 1mM Dithiothreitol (DTT), an antioxidant as negative control, or 100 µM Menadione, a free radical generator as positive control (Fig. 10, A and B).

In vitro Luciferase Assay

For the *in vitro* luciferase assay (Fig. 7), the transgenic zebrafish fibroblast cell line DAP49, which contains 3.1 kb of the *zfPeriod1* promoter driving the expression of luciferase, was used as published previously [10]. Amitrol (3-Amino-1, 2,4-triazole, 3-AT) was added from the beginning of the experiment in a concentration of 20 mM.

Statistics

Data are presented as mean ± SEM. To compare differences between two means, Student's t tests (two-tailed) were performed. To compare more than two means, data were analyzed using two-way analyses of variance (ANOVAs) followed by Holm-Sidak *post-hoc* tests and, in case of failed normality, Kruskal-Wallis one-way ANOVA on ranks. Significance was accepted for $p \leq 0.05$. Statistical analysis and cosinor analysis vs. straight line fit were performed using Graph Pad Prism 6.

Results and Discussion

The reciprocal interaction between the hypoxic signaling pathway and the circadian clock was described for the first time in the vertebrate model zebrafish [10, 28] and only

recently also found and characterized in more detail in mammals [5, 14, 15], which stresses the translational potential of the findings and the essential nature of the observed link, representing a fundamental aspect of eukaryotic cell biology. In this context, reduced oxygen tensions were found to dampen oscillation amplitudes of core clock genes in vertebrates including mammals through direct binding of Hypoxia Inducible Factor 1α (Hif-1α) to E-boxes of the genes *period1, period2* and *cryptochrome1,* all members of the negative limb of the core transcriptional translational feedback loop (TTFL) [10, 14, 15, 28, 30]. In turn, the expression of Hif-1α protein was shown to be clock controlled, and examples for the physiological relevance of the observed link between both pathways was likewise illustrated in zebrafish [28] and in mice [5, 15].

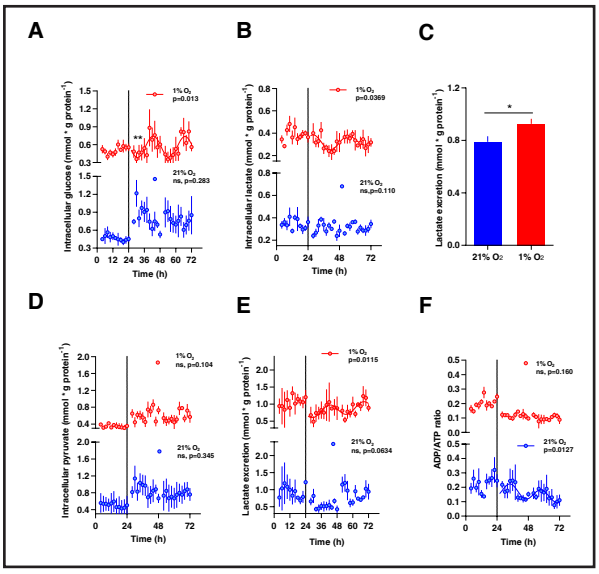

Fig. 2. Steady state concentrations of glycolytic key metabolites under normoxia and after hypoxia of two hours over three circadian cycles. A: short term hypoxia enhances circadian rhythmicity in intracellular glucose levels B: treatment with hypoxia for two hours enhances circadian rhythmicity of intracellular steady state lactate concentrations; C: Lactate production and excretion is increased in hypoxia treated cells; D: intracellular pyruvate concentrations do not follow a pronounced circadian rhythm under both conditions E: lactate excretion oscillates in a circadian manner after hypoxic treatment; F: cellular ADP/ATP ratios follow a circadian rhythm, which is attenuated/ablated after hypoxic treatment; asterisks mark significant differences between the groups; mean ± SEM; n=4; Two-way ANOVA , cosinor analysis vs. straight line fit were performed using Graph Pad Prism 6.

While the cell autonomous circadian time keeping of vertebrates has been largely focused on the transcriptional clock over the last years, some rather new models proposed by several authors [24-26] assigned increasing importance to metabolic rhythms for circadian time keeping, such as for example the peroxiredoxin oxidation cycles [16, 18-20]. Hence, we set out to investigate the effects of hypoxia on selected metabolites in a Zebrafish derived cell line which is directly light responsive [29], focusing thereby on key metabolites of glycolysis and markers of cellular redox environment over a period of three circadian cycles, one cycle under L/D (14/10), followed by two days under constant darkness for evaluation of the free running rhythm (Fig. 1, A). Since the hypoxia-induced decrease of the z*fper1* gene oscillation occurred earliest about 15 hours after onset of hypoxic treatment in whole animals [10], we presumed that some metabolic changes affecting cellular time keeping might happen already much earlier and therefore chose a rather short hypoxia incubation time, namely two hours of acute hypoxia, administrated immediately before each sampling time point. Consequently and of note, metabolic oscillations of cells under normoxia shown in the present study reflect endogenous rhythms of cellular metabolites, while those of hypoxia treated cells do not necessarily represent cell autonomous circadian rhythms, but rather constitute circadian variations of the cellular response to acute hypoxia.

Circadian variation of cellular metabolism in response to acute hypoxia

We found key metabolites of glycolysis such as glucose, pyruvate and lactate to oscillate rather erratically under normoxic control conditions, with highest levels of glucose and pyruvate during subjective day times (Fig. 2, A, B, and D). After administration of acute hypoxia concentrations of glycolytic intermediates revealed to be highly rhythmic,

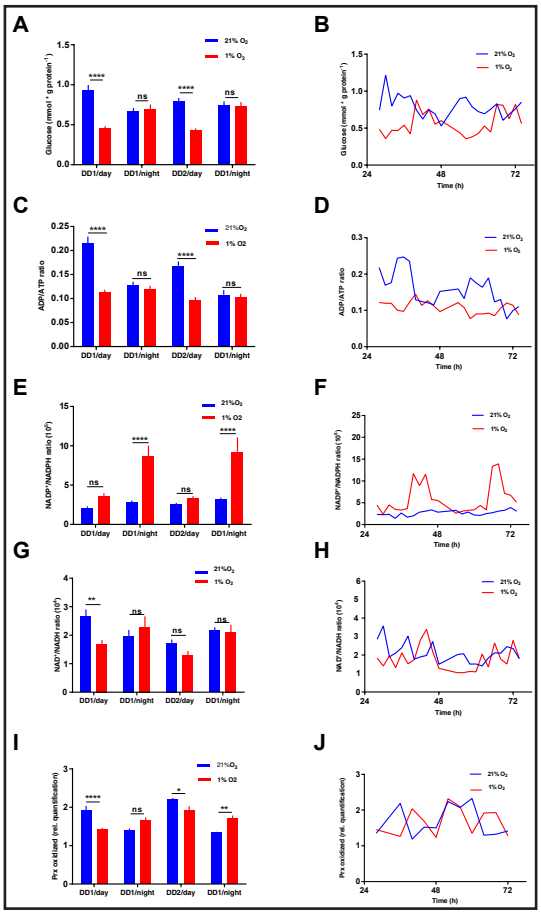

Fig. 3. Intracellular steady state concentrations of glucose and ADP/ATP ratios as markers for the glycolytic rhythms of cells under normoxia and following hypoxia of two hours during constant darkness; fluctuations of the three redox systems $NADP^+$/NADPH ratio, and NAD^+/NADH ratio as well as Prx_{ox} under normoxia and following hypoxia of two hours during constant darkness : A and B: the rhythm in steady state glucose concentration is reversed following hypoxia of two hours; C and D: ADP/ATP ratios of normoxic cells follow a circadian rhythm in phase with the oscillation of glucose; significant differences between normoxic and hypoxia treated cells can be found only during the subjective day times; E and F: the nocturnal $NADP^+$/NADPH ratio of hypoxia treated cells is highly increased, indicating an oxidized cellular state; G and H: only after hypoxic incubation of two hours the NAD^+/NADH ratio follows a circadian rhythm, in phase with the oscillation of the $NADP^+$/NADPH ratio; I and J: under normoxia oxidation cycles of Prx follow a circadian pattern as known from other species; acute hypoxia reduces the oscillation period to approximately 12 hours, so that during subjective night times hypoxia treated cells have increased levels of Prx_{ox} compared to cells under normoxia; asterisks mark significant differences between the groups; mean ± SEM; n= 72-132; Two-way ANOVA, Graph Pad Prism 6.

intracellular glucose and lactate following a clear circadian pattern with highest levels of glucose during the subjective night periods (Fig. 2, A and B; Fig. 3, A and B). Under both conditions, normoxia and following acute hypoxia of two hours, oscillation levels of glucose and pyruvate increased massively during constant darkness (Fig. 2, A and D). In addition, hypoxic cells revealed significantly reduced intracellular levels of glucose and pyruvate (Fig. 1, B and C), suggesting an increase in turn-over rate. To find an explanation for the increased substrate consumption of hypoxic cells we measured the production of lactate and found that intracellular steady state levels of lactate did not differ between both groups, whereas lactate excretion was enhanced in the latter (Fig. 2, C), following as well a clear circadian rhythm (Fig. 2, E), so that the highest release of lactate occurred during the subjective nights. Since glycolysis is the major source of ATP production we wanted to see if the opposed oscillations in glycolysis key metabolites after acute hypoxia had any influence on intracellular ADP/ATP ratios. Remarkably, we found ADP/ATP ratios of cells under normoxia to oscillate in a circadian manner (Fig. 2, F), which is the first evidence for cycling ADP/ATP pools in a metazoan cell line to our knowledge, and it is tempting to speculate that the observed circadian rhythms in cellular ADP/ATP ratios are functionally comparable to the phosphorylation cycles of the cyanobacterial clock [37]. In hypoxia treated cells the circadian ADP/ATP ratio oscillation was abolished, while total cellular ATP stores were increased (Fig. 1, D), as indicated also by the significantly lowered ADP/ATP ratios during subjective day times (Fig. 3, C and D). Higher levels of ATP can be either generated through an increased rate of glycolysis and mitochondrial respiration or through reduction of energy consuming processes under hypoxic conditions, known as metabolic depression. Increased stores of ATP are known to inhibit phosphofructokinase (PFK), the key rate limiting enzyme of glycolysis, leading to accumulating levels of fructose-6-phophate and glucose-6-phosphate, the latter of which

can be resynthesized from the former. This in turn enables the flow of glucose-6-phosphate into the pentose phosphate pathway (PPP), which produces the majority of NADPH reducing equivalents and pentoses for synthesis of nucleotides, depending on the demand of the cells. We therefore measured enzyme activities during the first day of constant darkness and found that nocturnal PFK activity was not altered after short term hypoxia, whereas the activity of glucose-6-phosphate dehydrogenase (G6PDH), the rate limiting enzyme of the PPP was significantly reduced in hypoxia treated cells during the early night, indicating that the glucose flux through the PPP was as well reduced (Fig. 4, B).

Acute hypoxia leads to a highly oxidized cellular environment during the night periods

As a next step we set out to investigate the effects of the moderately reduced flux through the PPP on the ratios of $NADP^+$/NADPH. We found clear circadian rhythms of $NADP^+$/NADPH ratios in normoxic as well as in hypoxia treated cells (Fig. 4, A), with phases and amplitudes not significantly differing from each other (oscillation amplitude increased by 3.89 ± 4.35 under hypoxia), but with significantly increased nocturnal $NADP^+$/NADPH ratios in hypoxia treated cells during the night phases (Fig. 3, E and F), where we also found the G6PDH activity to be reduced (Fig. 4, B), an enzyme which was only recently reported to regulate the circadian clock [27]. The cytosolic redox state of cells depends on the generation of reactive oxygen species as well as on the production of reducing equivalents such as NADPH, NADH or Prx_{red}. We therefore calculated the NAD^+/NADH ratios from pyruvate and lactate concentrations

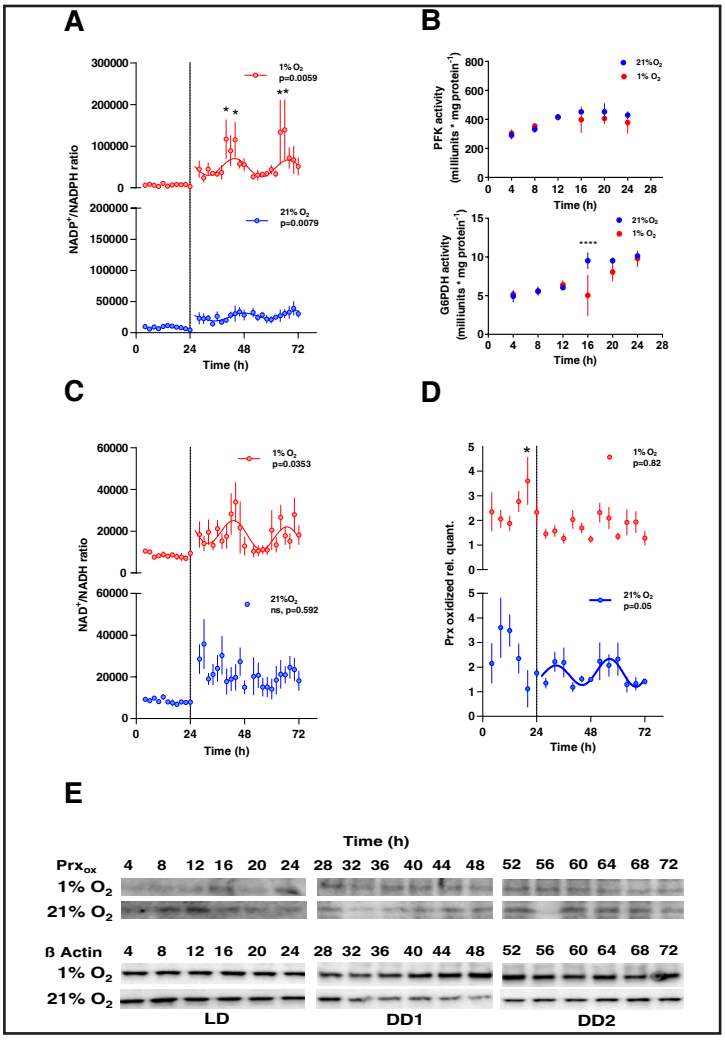

Fig. 4. Circadian profiles of the three redox systems NAD^+/NADH, $NADP^+$/NADPH ratios and Prx_{ox} under normoxia and after hypoxia of two hours; enzymatic activities of G6PDH and PFK during the first day of constant darkness: A: $NADP^+$/NADPH ratios oscillate with a circadian rhythm in normoxic and hypoxia treated cells; B: G6PDH and PFK activity during the first day of constant darkness: while the activity of PFK remains unaltered, the activity of G6PDH is significantly reduced in the early night after acute hypoxia; C: circadian profiles of NAD^+/NADH calculated after [33] from intracellular lactate and pyruvate levels: only hypoxia treated cells show a clear circadian oscillation; D and E: under normoxia Prx_{ox} oscillations follow a regular 24 hour rhythm, acute hypoxia leads to a reversal of the rhythm under LD and reduced periods of approximately 12 hours under constant darkness; asterisks mark significant differences between the groups, mean ± SEM; n=4; Two-way ANOVA, Cosinor analysis vs. straight line fit were performed using Graph Pad Prism 6.

after [33] and found that they followed as well a circadian pattern after administration of acute hypoxia, with highest levels during the subjective nights (Fig. 3, G and H; Fig. 4, C;). A circadian rhythm of Prx_{ox}, in contrast, was found only in normoxic control cells while after short term hypoxia and under constant darkness the oscillation period was reduced to approximately 12 hours, peaking thus twice during one circadian cycle (Fig. 4, D). During the first LD cycle circadian rhythms of Prx_{ox} were completely opposed between control and hypoxia treated cells, and in hypoxia treated cells under free run nocturnal Prx_{ox} levels were increased compared to normoxic cells (Fig. 3, I and J). Summarizing all results in a color coded table (Fig. 5), the alignment of the three investigated redox systems, the NAD^+/NADH ratio, the $NADP^+$/NADPH ratio and Prx_{redox}, after administration of short term hypoxia becomes evident: oscillation of the NAD^+/NADH ratio, which itself is driven by the hypoxia induced alterations in glycolytic activity (highest levels of intracellular glucose and lactate excretion coincide with lowest levels of ATP and NADH (Fig. 2, 3 and 4), starts to run in phase with the high amplitude oscillation of the $NADP^+$/NADPH ratio and the nocturnal peaks of Prx_{ox} (Fig. 4, A, C and D, Fig. 5), resulting finally in highly oxidized cellular environments during the subjective nights.

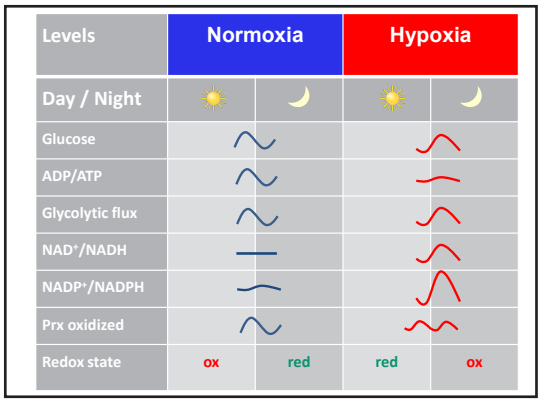

Fig. 5. Metabolic shift following hypoxia of two hours: Overview of steady state metabolite levels and redox ratio fluctuations in normoxic and hypoxia treated cells under constant darkness during the subjective day and night periods, resulting in opposed cellular redox states; data presented are based on Fig. 3.

Hypoxia reduces mitochondrial H_2O_2 but does not alter circadian rhythms of cytosolic H_2O_2

Hypoxia is known to involve altered ROS signaling and, though often controversially discussed [38, 39], it is meanwhile accepted that redox response to hypoxia can be cell-type and even cell compartment specific [40, 41] and that mitochondria are a source of ROS which is released to the cytosol in a controlled process [42, 43]. We therefore measured cytosolic as well as mitochondrial hydrogen peroxide levels under both conditions. Strikingly, cytosolic H_2O_2 oscillated in a circadian manner in both groups with identical amplitudes, phases and periods (Fig. 6, A, B and C). In contrast, mitochondrial H_2O_2 levels, which were recorded once in the middle of the day and once in the middle of the night during the first day of constant darkness, did not differ between day and night samples in both groups, but were significantly decreased in hypoxia treated cells (Fig. 6, D). For comparison, in a study on mammalian pulmonary artery smooth muscle cells (PASMCs) that used the same redox sensitive fluorescent protein sensors as in our study acute hypoxia induced a decrease in mitochondrial H_2O_2 as well, but an increase in cytosolic level instead [41]. Given this observation it is worth mentioning that, although the physiological ability to cope with hypoxia differs between hypoxia tolerant cyprinid fish and mammals, mitochondrial H_2O_2 levels in zebrafish fibroblasts and mammalian PASMCs alike respond very similar to acute hypoxic stress pointing towards a rather basic eukaryotic cellular response. We interpret the lower hydrogen peroxide in mitochondria upon hypoxia as prior mitochondrial release of H_2O_2 into the cytosol, but it might as well reflect reduced mitochondrial production of H_2O_2 under hypoxic conditions. A mitochondrial release of H_2O_2 might also explain the increased nocturnal levels of Prx_{ox} found after treatment with short term hypoxia, knowing that the release of mitochondrial H_2O_2 into the cytosol is controlled by PrxIII, [44, 45], the abundance of which constitutes a large portion of the peroxiredoxin isoform pool [46]. In order to test the actual impact of altered cellular H_2O_2 signaling on circadian time keeping we inhibited catalase, a major light-driven antioxidant enzyme regulating intracellular H_2O_2 levels [47],

with Amitrol and found that inhibition of the enzyme led to a lengthened period of the *period1* gene oscillation in the zebrafish *per1* luciferase reporter cell line DAP49 [48] (Fig. 7). The reset of the TTFL by H_2O_2 was described earlier by other groups [47, 49, 50], and a stable circadian period under hypoxic conditions was also reported for the rest-activity cycles of mice housed under normoxic (21% O_2) versus rhythmically reduced oxygen levels (21% O_2/16% O_2) [5]. We therefore conclude that the treatment with acute hypoxia leads to redistribution of intracellular H_2O_2 to the three reducing equivalents NADH, NADPH and Prx_{red} in order to keep the circadian oscillation of cytosolic H_2O_2 in phase, which otherwise might induce a change of the cell autonomous rhythm. A further reason for the redistribution of H_2O_2 to the reducing equivalents NADPH, NADH and Prx_{red} is in our opinion the generation of the highly oxidized nocturnal cellular state, which is in antiphase to the redox oscillation observed under normoxic control conditions (Fig. 3, 4 and 5). The binding affinity of the CLOCK /BMAL1 complex to the DNA is known to depend on the redox environment [23], so that the highly oxidized cellular environment during night times detected after acute hypoxia most probably interferes with the transcriptional feedback loop by weakening the binding affinity of the CLOCK /BMAL1 heterodimer, forming thus the basis for the hypoxia induced attenuation of the TTFL amplitude [10]. A treatment with hypoxia for two hours was also shown to not yet involve a significantly increased binding of Hif-1α to E-boxes of the *period1* gene in zebrafish cells [10], so that the Hif-1α induced repression of core clock genes during and after short term hypoxia most probably is not yet effective. In this context, the reduced G6PDH activity of hypoxia treated cells (Fig. 4, B) indicates that the PPP might have an important regulatory function for circadian time keeping also in the present experimental setup, by adding to the oxidized environment through reduced

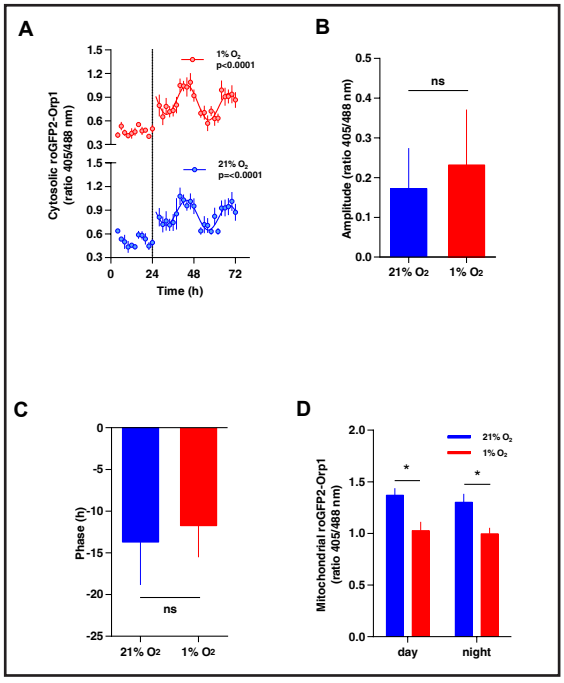

Fig. 6. Cytosolic and mitochondrial H_2O_2 in normoxic and hypoxia treated cells: A, B and C: circadian oscillations of cytosolic H_2O_2 levels do not differ between normoxic and hypoxia treated cells; mean ± SEM, n=5-6; D: mitochondrial H_2O_2 levels during the first day of constant darkness are significantly reduced in hypoxia treated cells, but do not differ between night and day; asterisks mark significant differences (mean ± SEM, n=3; t-test); Cosinor analysis vs. straight line fit were performed using Graph Pad Prism 6.

Fig. 7. In Vitro Luciferase Assay. Long-term zfper1 promoter activity driving luciferase in the Zebrafish cell line DAP49; cells incubated with the inhibitor Amitrol (3-Amino-1,2,4-triazole, 3-AT) at 20 mM, which inhibits the activity of catalase, experience a phase advance of the zfper1 oscillation; mean values ± SEM (n=8). cosinor analysis vs. straight line fit was performed using Graph Pad Prism 6; asterisks mark significant differences between the groups.

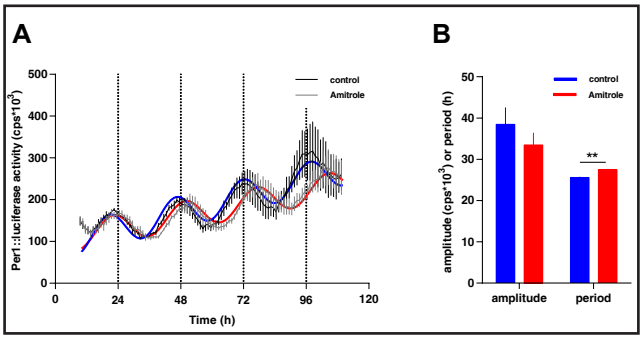

production of reducing equivalents, hence confirming the role of glucose catabolism in the regulation of the TTFL amplitude reported previously [27, 50]. However, our results also implicate that a cellular timekeeping mechanism apart from the transcriptional clock is obviously quite robust against the stress of reduced oxygen tensions, in line with a recent review [50].

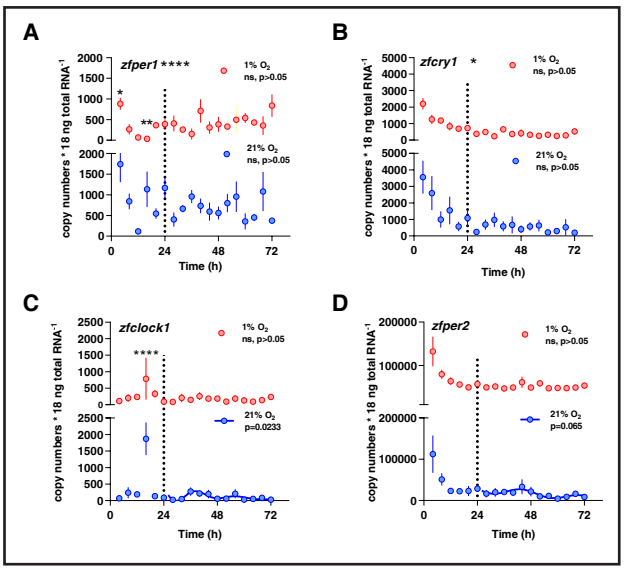

Fig. 8. Impact of short term hypoxia on the TTFL: A and B: expression levels of zfper1 and zfcry1 are significantly reduced in hypoxia treated cells; C: acute hypoxia significantly decreases the mRNA copy number of zfclock1 in the early night of the first L/D cycle, the circadian oscillation of zfclock1 is attenuated/ablated after hypoxic treatment of two hours; D: the circadian oscillation of zfper2 is attenuated/ablated following hypoxia of two hours; B and D: zfcry1 and zfper2 are two light driven genes of Zebrafish, indicated by the sharp decreases in their mRNA expression under constant darkness; asterisks mark significant differences between the groups; mean ± SEM; n=3-4; Two-way ANOVA, cosinor analysis vs. straight line fit were performed using Graph Pad Prism 6.

Acute hypoxia attenuates the transcriptional clock

Chronic hypoxia is known to reduce the oscillation amplitudes of specific clock genes [10, 14, 15, 28]. To confirm the hypoxia induced attenuation of the TTFL also for the present experimental setup using acute hypoxia we screened mRNA oscillation of core clock genes and found that expression levels of the clock genes *period1b* (*per1*) and *cryptochrome1aa* (*cry1*) were significantly reduced, as was the copy number of *clock1a* (*clock1*) recorded in the early LD night (Fig. 8, A, B and C). In addition, circadian oscillations of *clock1* and *period2* mRNA ceased after administration of acute hypoxia (Fig. 8, C and D). Besides, mRNA expression levels of the two light responsive genes *cry1* and *per2,* both of which are known to be crucial for the light induced reset of the circadian clock in zebrafish [47, 51], decreased massively under constant darkness (Fig. 8, B and D), corresponding therewith to previous reports [47, 52]. Hence, the effects of short term hypoxia on the transcriptional clock were comparable to those reported earlier for chronic hypoxia [10]. We therefore conclude that it would be of no benefit for cells and tissues to immediately lose track of time when oxygen tensions decrease (eventually only timely restricted), and that cells and tissues compensate the hypoxia induced attenuated rhythms of peripheral clocks with enhanced metabolic rhythmicity on the one hand and a stable oscillation of cytosolic H_2O_2 on the other in order to keep the cell autonomous rhythm.

Increased levels and amplitudes of metabolic cycles under constant darkness

Intriguingly, basic levels of five measured metabolites significantly changed at the "subjective dawn" of the first day under constant darkness, when cells seemed to anticipate "light on" after synchronization over two circadian cycles to an L/D rhythm of 14/10. This phenomenon, which was initially thought to be an artefact, was observed in normoxic and hypoxia treated wildtype Z3 cells, as well as in the genetically modified RoGFP2 Z3 cell line. Highly increased mean levels were detected for intracellular glucose and pyruvate (Fig. 2, A and D), for the NAD^+/ NADH and $NADP^+$/NADPH ratios (Fig. 4, A and C), for the ATP/ADP ratio (reversed, Fig. 2, F) and for cytosolic H_2O_2 in the transgenic RoGFP2 Z3 cell line (Fig. 6, A). Of note, the in phase oscillation of all three redox systems after acute hypoxia was observed

as well only during constant darkness, when oscillations and /or expression levels of both light driven clock genes *per2* and *cry1* [51] were severely reduced, and the realignment of the three redox systems might therefore also compensate for the loss of the external timing cue light, just as the increased levels and oscillations of metabolites observed under constant darkness.

Hif-1α protein follows a circadian rhythm under normoxic control conditions

Since Hif-1α regulates the expression of many glycolytic enzymes (phosphofructokinase PFK, pyruvate kinase PK, lactate dehydrogenase LDH, hexokinase HK) and glucose transporters (Glut1 and Glut3) [53], we considered Hif-1α as primarily responsible for the shift of the glycolytic activity into the night periods and thus also for the increased in phase oscillations of the three redox systems. In addition, Hif-1α was only recently demonstrated to be essential for the reset of the circadian clock upon applied oxygen rhythms, by using an siRNA approach in a mouse model [5]. Measurement of basic mRNA and protein levels of Hif-1α in our study revealed mRNA expression patterns of *hif-1α* to oscillate rather unsteadily under both conditions (Fig. 9, A) and application of acute hypoxia did not result in any significant differences regarding the abundance of hif-1α mRNA copy numbers between control and hypoxia treated cells. In contrast, Hif-1α protein followed a clear circadian rhythm under control conditions, as it was reported only recently by [5], who showed that normoxic Hif-1α protein rhythms were based on daily rhythms in tissue oxygenation [5]. Treatment of cells with acute hypoxia increased Hif-1α protein levels significantly, as expected (Fig. 9, B and C), and did not follow a clear circadian rhythm, again in accordance with the situation described in mammals earlier [5], stressing again the conserved nature of the mutual link between both pathways.

Conclusion

In summary, our study supports the idea that Hif-1α is required and responsible for the observed acute as well as known chronic hypoxia induced effects on the circadian clock. Since circadian rhythms of cytosolic H_2O_2 remain absolutely unaffected by the hypoxia induced metabolic and transcriptional changes, a cellular timekeeping mechanism apart from the transcriptional clock is obviously quite robust against the stress of reduced oxygen tensions. Reversely, Hif-1α, which has been demonstrated to be tightly clock controlled itself, is most probably mainly responsible for the orchestration of metabolic alterations, which lead to a time-of-day dependent variation in the cellular response to hypoxia, but also allow for the hypoxia induced attenuation of the circadian clock by altering the cellular redox state, as

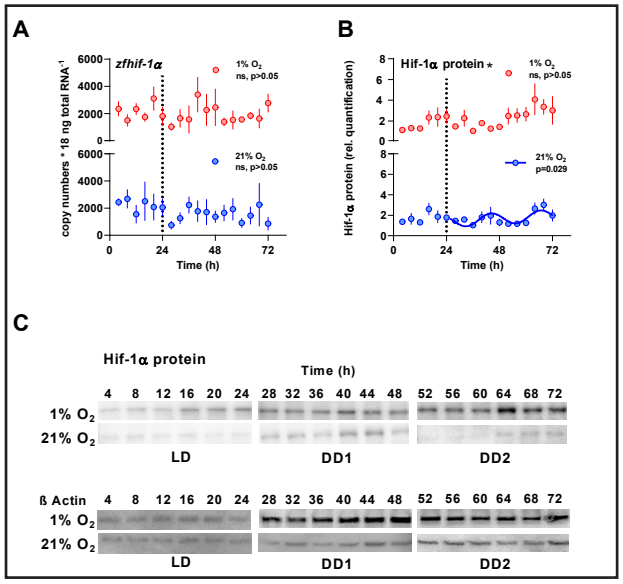

Fig. 9. Circadian profiles of zfhif-1α mRNA and Hif-1α protein under normoxia and following hypoxia of two hours: A: zfhif-1α mRNA expression does not follow a clear 24 hour rhythm under both conditions; B and C: under normoxia Hif-1α protein levels oscillate in a circadian manner, after hypoxia of two hours circadian rhythmicity is lost and protein quantities are significantly increased; asterisks mark significant differences between the groups; mean ± SEM; n=3-4; Two-way ANOVA, cosinor analysis vs. straight line fit were performed using Graph Pad Prism 6.

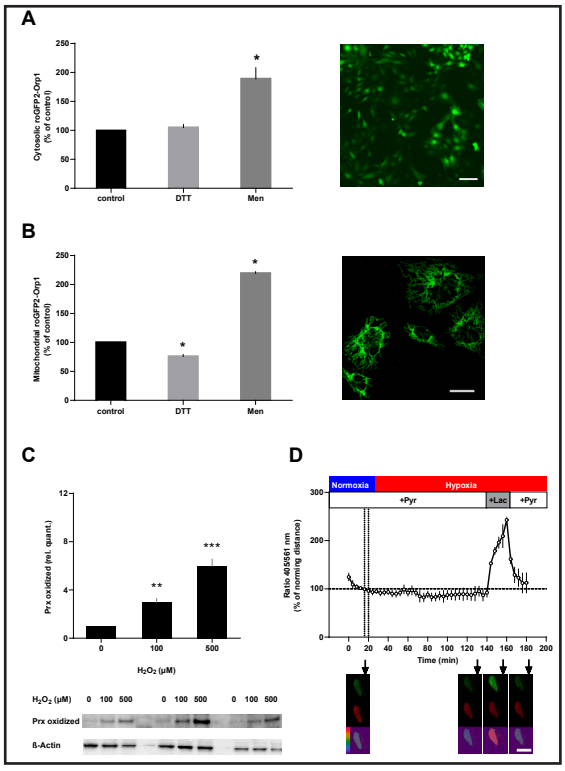

Fig. 10. A and B: responsiveness of the roGFP2-ORP1 fluorescent protein sensor in the cytosolic (A) or mitochondrial (B) measurement setup was confirmed by applying either 1mM Dithiothreitol (DTT), an antioxidant as negative control, or 100 µM Menadione, a free radical generator as positive control; Significant differences (ANOVA, P< 0,05) between the treatment groups are shown (mean ± SEM; A: n=6; B: n=3); image A: Z3 cells with stable transfection of roGFP2-ORP1 in the cytosol, image B: Z3 cells with stable transfection of roGFP2-ORP1 localized to the mitochondria. Scale bar: 25 µm; C: Prx oxidized positive controls: Prx oxidized increases significantly with increasing concentrations of H_2O_2 in the medium, while ß-actin does not (mean ± SEM, n=3; one way ANOVA, Graph Pad Prism 6); D: equilibrium experiment: relative cytosolic levels of NADH for determination of the equilibrium state of the cytosolic reaction Pyruvate + NADH + H^+ <—> Lactate + NAD^+ were measured with the Peredox-mCherry sensor transiently transfected in Z3 cells. The sensor was excited at two wavelengths (Ex1 405 nm, Em1 500-550 nm, Ex2 561 nm, Em2 600–650 nm) to produce two images which were used for ratiometric image analysis; cells under normoxia and after two hours of hypoxia do not differ significantly in their ratio; at the end of the experiment imaging buffer containing 5 mM galactose and 5 mM pyruvate was exchanged to a buffer containing 5 mM galactose and 5 mM lactate to serve as a positive control for the sensor in a non-equilibrium state (high NADH concentration); inserts show a representative cell at 4 different timepoints (20 min, 135 min, 155 min, 180 min) in green and red emission and the ratio image in glow scale (ratio values 0-2); Scale bar: 40 µm; mean ± SEM (n=3); asterisks mark significant differences between the groups.

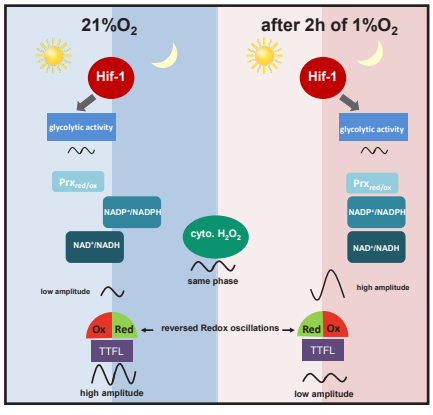

Fig. 11. Under normoxia glycolytic activity occurs predominantly during day time, controlled to a large extent by Hypoxia Inducible Factor 1 alpha (Hif-1α), which regulates the expression of many glycolytic enzymes such as phosphofructokinase, pyruvate kinase, lactate dehydrogenase, hexokinase and glucose transporters. Markers and effectors of the cellular redox system such as $NADP^+$/NADPH ratio and oxidations cycles of Peroxiredoxins (Prx) oscillate in a circadian manner, while the NAD^+/NADH ratio does not follow a 24 hour rhythm. Oxidation maxima and minima of their oscillations occur during different times of one circadian cycle. After acute hypoxia of two hours: administration of hypoxia for two hours shifts highest maxima of glycolytic activity into the night periods, leading to the alignment of the NAD^+/NADH ratio with the high amplitude oscillation of the $NADP^+$/NADPH ratio and nocturnal Prx_{ox} and, as a result, to a highly oxidized cellular environment during the night. While cytosolic H_2O_2 oscillations (middle) remain completely unaffected and keep amplitude and phase also after treatment with acute hypoxia, the TTFL is already attenuated comparable to the effect of chronic hypoxia on the transcriptional clock.

shown in the model (Fig. 11). We therefore think that our study represents a completely new aspect of the intimate, mutual and conserved link between the circadian clock and hypoxic signaling, by integrating physiological processes, which obviously precede the direct transcriptional repression of core clock genes through Hif-1α, and might therefore be of great value for basic eukaryotic cell biology.

Acknowledgements

Work was supported by the following grants: Tiroler Wissenschaftsfond TWF, Project number GZL. 0404/2017 for M.P. and Advancement of junior researchers #226115, University Innsbruck, for A.M.S.. We thank Nathalie Oberthaler, Mag. Birgit Fiechtner, MSc Valentina Dikova and Julia Nagy for their help in the lab and Daniela Rainer for her idea on the two hours hypoxic incubation. Our special thanks goes to Dr. John O`Neill for constructive criticism from the chronobiological point of view and help with cosinor analysis.

A.M.S. established and performed the mitochondrial and cytosolic H_2O_2 measurements, supervised all cell culture experiments and the circadian sampling schedules and did the *in vitro* Luciferase Assay as well as the enzymatic measurements. B.J. and M.P. did most of the circadian sampling, the Prx western blots and the metabolic measurements. B.A.P. helped with protein sampling and the Prx western blots. B.P. had fruitful discussions about cellular physiology with M.E. and revised the manuscript. M.E. designed the study, analyzed and interpreted the data, and wrote the manuscript.

Disclosure Statement

No conflict of interests exists.

References

1 Gorr TA, Gassmann M, Wappner P: Sensing and responding to hypoxia via HIF in model invertebrates. J Insect Physiol 2006;52:349-364.
2 Semenza GL: HIF-1: mediator of physiological and pathophysiological responses to hypoxia. J Appl Physiol 2000;88:1474-1480.
3 Shen C, Nettleton D, Jiang M, Kim SK, Powell-Coffman JA: Roles of the HIF-1 hypoxia-inducible factor during hypoxia response in Caenorhabditis elegans. J Biol Chem 2005;280:20580-20588.
4 Nikinmaa M, Rees BB: Oxygen-dependent gene expression in fishes. Am J Physiol Regul Integr Comp Physiol 2005;288:R1079-R1090.
5 Adamovich Y, Ladeuix B, Golik M, Koeners MP, Asher G: Rhythmic Oxygen Levels Reset Circadian Clocks through HIF1alpha. Cell Metab 2016.
6 Bosco G, Ionadi A, Panico S, Faralli F, Gagliardi R, Data P, Mortola JP: Effects of hypoxia on the circadian patterns in men. High Alt Med Biol 2003;4:305-318.
7 Chilov D, Hofer T, Bauer C, Wenger RH, Gassmann M: Hypoxia affects expression of circadian genes PER1 and CLOCK in mouse brain. FASEB J 2001;15:2613-2622.
8 Coste O, Beaumont M, Batejat D, Beers PV, Touitou Y: Prolonged mild hypoxia modifies human circadian core body temperature and may be associated with sleep disturbances. Chronobiol Int 2004;21:419-433.
9 Coste O, van BP, Touitou Y: Hypoxia-induced changes in recovery sleep, core body temperature, urinary 6-sulphatoxymelatonin and free cortisol after a simulated long-duration flight. J Sleep Res 2009;18:454-465.
10 Egg M, Koblitz L, Hirayama J, Schwerte T, Folterbauer C, Kurz A, Fiechtner B, Most M, Salvenmoser W, Sassone-Corsi P, Pelster B: Linking Oxygen to Time: The Bidirectional Interaction Between the Hypoxic Signaling Pathway and the Circadian Clock. Chronobiol Int 2013;30:510-529.

11 Ghorbel MT, Coulson JM, Murphy D: Cross-talk between hypoxic and circadian pathways: cooperative roles for hypoxia-inducible factor 1alpha and CLOCK in transcriptional activation of the vasopressin gene. Mol Cell Neurosci 2003;22:396-404.
12 Mazzoccoli G, De CA, Piepoli A, Vinciguerra M: The circadian clock and the hypoxic response pathway in kidney cancer. Tumour Biol 2014;35:1-7.
13 Mortola JP, Seifert EL: Hypoxic depression of circadian rhythms in adult rats. J Appl Physiol 2000;88:365-368.
14 Peek CB, Levine DC, Cedernaes J, Taguchi A, Kobayashi Y, Tsai SJ, Bonar NA, McNulty MR, Ramsey KM, Bass J: Circadian Clock Interaction with HIF1alpha Mediates Oxygenic Metabolism and Anaerobic Glycolysis in Skeletal Muscle. Cell Metab 2016;25:86-92.
15 Wu Y, Tang D, Liu N, Xiong W, Huang H, Li Y, Ma Z, Zhao H, Chen P, Qi X, Zhang EE: Reciprocal Regulation between the Circadian Clock and Hypoxia Signaling at the Genome Level in Mammals. Cell Metab 2016;25:73-85.
16 Edgar RS, Green EW, Zhao Y, van OG, Olmedo M, Qin X, Xu Y, Pan M, Valekunja UK, Feeney KA, Maywood ES, Hastings MH, Baliga NS, Merrow M, Millar AJ, Johnson CH, Kyriacou CP, O'Neill JS, Reddy AB: Peroxiredoxins are conserved markers of circadian rhythms. Nature 2012;485:459-464.
17 O'Neill JS, Reddy AB: Circadian clocks in human red blood cells. Nature 2011;469:498-503.
18 O'Neill JS, van OG, Dixon LE, Troein C, Corellou F, Bouget FY, Reddy AB, Millar AJ: Circadian rhythms persist without transcription in a eukaryote. Nature 2011;469:554-558.
19 Causton HC, Feeney KA, Ziegler CA, O'Neill JS: Metabolic Cycles in Yeast Share Features Conserved among Circadian Rhythms. Curr Biol 2015;25:1056-1062.
20 Rhee SG: Overview on Peroxiredoxin. Mol Cells 2016;39:1-5.
21 Nakahata Y, Sahar S, Astarita G, Kaluzova M, Sassone-Corsi P: Circadian control of the NAD+ salvage pathway by CLOCK-SIRT1. Science 2009;324:654-657.
22 Ramsey KM, Yoshino J, Brace CS, Abrassart D, Kobayashi Y, Marcheva B, Hong HK, Chong JL, Buhr ED, Lee C, Takahashi JS, Imai S, Bass J: Circadian clock feedback cycle through NAMPT-mediated NAD+ biosynthesis. Science 2009;324:651-654.
23 Rutter J, Reick M, Wu LC, McKnight SL: Regulation of clock and NPAS2 DNA binding by the redox state of NAD cofactors. Science 2001;293:510-514.
24 Bass J, Takahashi JS: Circadian rhythms: Redox redux. Nature 2011;469:476-478.
25 Bass J: Circadian topology of metabolism. Nature 2012;491:348-356.
26 Rey G, Reddy AB: Connecting cellular metabolism to circadian clocks. Trends Cell Biol 2013;23:234-241.
27 Rey G, Valekunja UK, Feeney KA, Wulund L, Milev NB, Stangherlin A, Ansel-Bollepalli L, Velagapudi V, O'Neill JS, Reddy AB: The Pentose Phosphate Pathway Regulates the Circadian Clock. Cell Metab 2016;24:462-473.
28 Egg M, Paulitsch M, Ennemoser Y, Wustenhagen A, Schwerte T, Sandbichler AM, Fiechtner B, Koblitz L, Prem C, Pelster B: Chronodisruption increases cardiovascular risk in zebrafish via reduced clearance of senescent erythrocytes. Chronobiol Int 2014;31:680-689.
29 Tamai TK, Carr AJ, Whitmore D: Zebrafish circadian clocks: cells that see light. Biochem Soc Trans 2005;33:962-966.
30 Pelster B, Egg M: Multiplicity of hypoxia inducible transcription factors and their connection to the circadian clock in the zebrafish. Physiological and Biochemical Zoology. In press.
31 Bergmeyer HU: Methoden der enzymatischen Analyse. Verlag Chemie, Weinheim, 1974.
32 Rost FWD: Fluorescence Microscopy; Cambridge University Press, New York, NY., 1995.
33 Sun F, Dai C, Xie J, Hu X: Biochemical issues in estimation of cytosolic free NAD/NADH ratio. PLoS One 2012;7:e34525.
34 Hung YP, Albeck JG, Tantama M, Yellen G: Imaging cytosolic NADH-NAD(+) redox state with a genetically encoded fluorescent biosensor. Cell Metab 2011;14:545-554.
35 Sandbichler AM, Aschberger T, Pelster B: A method to evaluate the efficiency of transfection reagents in an adherent zebrafish cell line. Biores Open Access 2013;2:20-27.
36 Gutscher M, Sobotta MC, Wabnitz GH, Ballikaya S, Meyer AJ, Samstag Y, Dick TP: Proximity-based protein thiol oxidation by H2O2-scavenging peroxidases. J Biol Chem 2009;284:31532-31540.
37 Nakajima M, Imai K, Ito H, Nishiwaki T, Murayama Y, Iwasaki H, Oyama T, Kondo T: Reconstitution of circadian oscillation of cyanobacterial KaiC phosphorylation *in vitro*. Science 2005;308:414-415.

38 Guzy RD, Schumacker PT: Oxygen sensing by mitochondria at complex III: the paradox of increased reactive oxygen species during hypoxia. Exp Physiol 2006;91:807-819.
39 Sgarbi G, Gorini G, Costanzini A, Barbato S, Solaini G, Baracca A: Hypoxia decreases ROS level in human fibroblasts. Int J Biochem Cell Biol 2017;88:133-144.
40 Kaludercic N, Deshwal S, Di LF: Reactive oxygen species and redox compartmentalization. Front Physiol 2014;5:285.
41 Waypa GB, Marks JD, Guzy R, Mungai PT, Schriewer J, Dokic D, Schumacker PT: Hypoxia triggers subcellular compartmental redox signaling in vascular smooth muscle cells. Circ Res 2010;106:526-535.
42 Chandel NS: Mitochondria as signaling organelles. BMC Biol 2014;12:34.
43 Sabharwal SS, Schumacker PT: Mitochondrial ROS in cancer: initiators, amplifiers or an Achilles' heel? Nat Rev Cancer 2014;14:709-721.
44 Kil IS, Ryu KW, Lee SK, Kim JY, Chu SY, Kim JH, Park S, Rhee SG: Circadian Oscillation of Sulfiredoxin in the Mitochondria. Mol Cell 2015;59:651-663.
45 Toledano MB, Delaunay-Moisan A: Keeping Oxidative Metabolism on Time: Mitochondria as an Autonomous Redox Pacemaker Animated by H2O2 and Peroxiredoxin. Mol Cell 2015;59:517-519.
46 Cox AG, Winterbourn CC, Hampton MB: Mitochondrial peroxiredoxin involvement in antioxidant defence and redox signalling. Biochem J 2009;425:313-325.
47 Hirayama J, Cho S, Sassone-Corsi P: Circadian control by the reduction/oxidation pathway: Catalase represses light-dependent clock gene expression in the zebrafish. Proceedings of the National Academy of Sciences 2007;104:15747-15752.
48 Vallone D, Gondi SB, Whitmore D, Foulkes NS: E-box function in a period gene repressed by light. Proc Natl Acad Sci U S A 2004;101:4106-4111.
49 Stangherlin A, Reddy AB: Regulation of circadian clocks by redox homeostasis. J Biol Chem 2013;288:26505-26511.
50 Putker M, O'Neill JS: Reciprocal Control of the Circadian Clock and Cellular Redox State - a Critical Appraisal. Mol Cells 2016;39:6-19.
51 Tamai TK, Young LC, Whitmore D: Light signaling to the zebrafish circadian clock by Cryptochrome 1a. Proc Natl Acad Sci U S A 2007;104:14712-14717.
52 Pando MP, Pinchak AB, Cermakian N, Sassone-Corsi P: A cell-based system that recapitulates the dynamic light-dependent regulation of the vertebrate clock. Proc Nat Acad Sci U S A 2001;98:10178-10183.
53 Porporato PE, Dhup S, Dadhich RK, Copetti T, Sonveaux P: Anticancer targets in the glycolytic metabolism of tumors: a comprehensive review. Front Pharmacol 2011;2:49.